arXiv:1303.1974v1 [cond-mat.supr-con] 8 Mar 2013

Rashba spin-orbit coupling effects in quasiparticle interference of non-centrosymmetric superconductors

Alireza Akbari and Peter Thalmeier
Max Planck Institute for the Chemical Physics of Solids, D-01187 Dresden, Germany

(Dated: March 11, 2013)

The theory of quasiparticle interference (QPI) for non-centrosymmetric (NCS) superconductors with Rashba spin-orbit coupling is developed using T-matrix theory in Born approximation. We show that qualitatively new effects in the QPI pattern originate from the Rashba spin-orbit coupling: The resulting spin coherence factors lead to a distinct difference of charge- and spin- QPI and to an induced spin anisotropy in the latter even for isotropic magnetic impurity scattering. In particular a cross - QPI appears describing spin oscillation pattern due to nonmagnetic impurity scattering which is directly related to the Rashba vector. We apply our theory to a 2D model for the NCS heavy fermion unconventional superconductor $\mathrm{CePt_3Si}$ and discuss the new QPI features for a gap model with accidental node lines due to its composite singlet-triplet nature.

PACS numbers: 74.20.Rp, 74.55.+v, 74.70.Tx

The determination of gap symmetry in unconventional superconductors (SC) is a persistent problem. Most useful methods for its investigation are ARPES experiments [1], specific heat and thermal transport measurements under rotating field [2] and the use of STM-based quasiparticle interference technique (QPI) which utilizes the ripples in electronic density generated by random surface impurities [3–5]. In the cuprate and iron pnictides the former is readily applicable but sofar not for heavy fermion unconventional superconductors where SC gaps are only in the meV range. In this case the last two methods are more powerful. QPI technique has recently been proposed to discriminate between different d-wave pairing states in 115 systems [6] and successfully demonstrated for $\mathrm{CeCoIn_5}$ [7]. Before it was also used to investigate the hidden order state of $\mathrm{URu_2Si_2}$ [8–10].

Here we propose the application of QPI to inversion symmetry-breaking, non-centrosymmetric (NCS) superconductors, notably the tetragonal heavy fermion 131 and 113 compounds [11] like $\mathrm{CePt_3Si}$ [12] and $\mathrm{CeRhSi_3}$ [13]. We develop the QPI theory for the case of mixed singlet-triplet gap under the presence of Rashba-type spin-orbit coupling. We show that a wealth of new QPI features is to be expected: i) Distinct differences in the charge- and spin- QPI due to the effect of Rashba coherence factors. ii) Likewise Rashba - induced anisotropies in the spin- QPI even for isotropic magnetic impurity scattering. iii) A new kind of cross- QPI where scattering by *nonmagnetic* (charge) impurities leads to spin density pattern directly related to the non-zero Rashba vector (and vice versa). Finally the expected gap nodes in NCS superconductors are generally not on symmetry positions but determined by the ratio of singlet and triplet amplitudes. QPI can give important information on the position of these accidental nodes. We use a weak coupling BCS theory for the NCS superconductor with a 2D model Fermi surface appropriate for 131 compounds. We employ Nambu Green's function technique and T-matrix theory in Born approximation to calculate the quasiparticle interference spectra and discuss their new features as compared to centrosymmetric unconventional superconductors.

The BCS model for non-centrosymmetric superconductors is given by [14–16]

$$\mathcal{H}_{SC} = \sum_{\mathbf{k}\sigma\sigma'} \left[(\varepsilon_{\mathbf{k}} - \mu)\sigma_0 + \mathbf{g}_{\mathbf{k}} \cdot \boldsymbol{\sigma}\right]_{\sigma\sigma'} c^{\dagger}_{\mathbf{k}\sigma} c_{\mathbf{k}\sigma'} + \frac{1}{2}\sum_{\mathbf{k}\sigma\sigma'} (\Delta^{\sigma\sigma'}_{\mathbf{k}} c^{\dagger}_{-\mathbf{k}\sigma} c^{\dagger}_{\mathbf{k}\sigma'} + H.c.). \quad (1)$$

Here $\varepsilon_{\mathbf{k}} = 2t_1(\cos k_x + \cos k_y) + 4t_2 \cos k_x \cos k_y$ is the kinetic energy with respect to chemical potential μ where t_1 are next and t_2 next nearest neighbor hopping. Furthermore $\mathbf{g}_{\mathbf{k}} = -\mathbf{g}_{-\mathbf{k}}$ defines the antisymmetric Rashba term due to broken inversion symmetry [17]. Therefore the superconducting 2×2 gap matrix $\Delta_{\mathbf{k}} = [\psi_{\mathbf{k}}\sigma_0 + \mathbf{d}_{\mathbf{k}} \cdot \boldsymbol{\sigma}]i\sigma_y$ has an even singlet ($\psi_{\mathbf{k}}$) as well as odd triplet ($\mathbf{d}_{\mathbf{k}}$) components. The latter must be aligned with the Rashba vector $\mathbf{d}_{\mathbf{k}} = \phi_0 \mathbf{g}_{\mathbf{k}}$ to avoid destruction by pairbreaking [18]. Here $\boldsymbol{\sigma} = (\sigma_x, \sigma_y, \sigma_z)$ denotes the Pauli matrices. Diagonalization of the model leads to an effective two band superconductor on the Rashba split bands ($\xi = \pm 1$) given by $\epsilon_{\mathbf{k}\xi} = \varepsilon_{\mathbf{k}} - \mu + \xi|\mathbf{g}_{\mathbf{k}}|$ that have split Fermi surfaces (FS) and opposite helical spin polarizations as well as different superconducting gaps $\Delta_{\mathbf{k}\xi} = \psi_{\mathbf{k}} + \xi|\mathbf{d}_{\mathbf{k}}|$. For concreteness we employ a 2D model for the tetragonal Ce- based 131 compounds [19, 20]. The possible influence of magnetic order [21] is not discussed here.

In this class $\mathbf{g}_{\mathbf{k}} = g(\sin k_y, -\sin k_x, 0)$ is in the tetragonal plane. The resulting Rashba-split bands (inset) and density of states (DOS) (in the SC state) are shown in Fig. 1a and the electron-type Fermi surface around the M(π, π) points in Fig. 1b. The split constant-energy surfaces ($\omega > 0$) are presented in Fig. 1b,c. It is known from thermal conductivity [22] that the superconducting gap has line nodes. To achieve nodes on the M-point Fermi surface we use an extended s-wave [18] form for

$\psi_{\mathbf{k}}$ and $\mathbf{d}_{\mathbf{k}}$ as before. This leads to the two distinct gaps $\Delta_{\mathbf{k}\xi} = \psi_0 + \psi_1(\cos k_x + \cos k_y) + \xi\phi_0 g_0(\sin k_x^2 + \sin k_y^2)^{\frac{1}{2}}$ on the Rashba-split Fermi surfaces $\epsilon_{\mathbf{k}\xi} = \mu$ with quasiparticle energies $E_{\mathbf{k}\xi} = [\epsilon_{\mathbf{k}\xi}^2 + \Delta_{\mathbf{k}\xi}^2]^{\frac{1}{2}}$. The gap zeroes are shown as dashed lines in Fig. 1b-d. Nodes (node lines in 3D) appear on the FS for the $E_{\mathbf{k}-}$ quasiparticle sheet but not for $E_{\mathbf{k}+}$. Their position is accidental, i.e. determined by the fine tuning of singlet and triplet amplitudes ψ_1 and ϕ_0. The evolution of constant energy surfaces in the SC state is shown in Fig. 1e-h. A few wave vectors $\mathbf{q}_i$ connecting high curvature points close to nodal positions that will appear prominently in QPI spectra for small ω are shown in Fig. 1e. For larger ω (Fig. 1h) connected FS sheets reappear. For the calculation of the QPI pattern we use the normal and anomalous matrix Greens functions of the unperturbed system $G = G_+\sigma_0 + G_-(\hat{\mathbf{g}}_{\mathbf{k}} \cdot \boldsymbol{\sigma})$ and $F = [F_+\sigma_0 + F_-(\hat{\mathbf{g}}_{\mathbf{k}} \cdot \boldsymbol{\sigma})]i\sigma_y$, respectively, where ($\hat{\mathbf{g}}_{\mathbf{k}} = \mathbf{g}_{\mathbf{k}}/|\mathbf{g}_{\mathbf{k}}|$).

$$G_\pm(\mathbf{k}, i\omega_n) = \frac{1}{2}\sum_\xi \left\{ \begin{array}{c} 1 \\ \xi \end{array} \right\} \frac{(i\omega_n + \epsilon_{\mathbf{k}\xi})}{[(i\omega_n)^2 - E_{\mathbf{k}\xi}^2]},$$
$$F_\pm(\mathbf{k}, i\omega_n) = \frac{1}{2}\sum_\xi \left\{ \begin{array}{c} 1 \\ \xi \end{array} \right\} \frac{\Delta_{\mathbf{k}\xi}}{[(i\omega_n)^2 - E_{\mathbf{k}\xi}^2]}. \qquad (2)$$

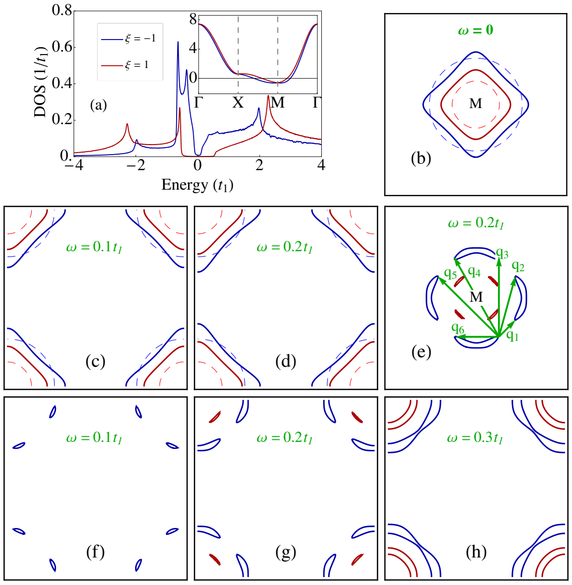

FIG. 1. a) Electronic density of states (DOS) of Rashba bands ($\xi = \pm 1$) in the SC state. (inset: 2D band structure along ΓXMΓ with $t_2 = 0.35t_1, g = 0.2t_1$, and $\mu = -2t_1$). b) Normal state electron Fermi surface around M point. Dashed lines indicate nodes of gap functions $\Delta_{\mathbf{k}\xi}$ with parameters: $\psi_0 = 2t_1$, $\psi_1 = t_1$, and $\phi_0 = 0.65t_1$ (also in subsequent figures). c) and d) show spectral functions in the normal state for different energies ω. e) Spectral function for the superconducting state around M point. $\mathbf{q}_i$ are prominent scattering vectors defining the QPI patterns (c.f. Figs.3e, 4f). f-h) Spectral function for the superconducting state for different ω.

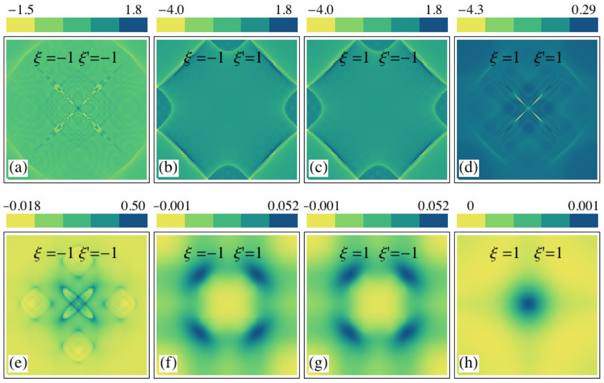

FIG. 2. The individual charge- QPI ($\Lambda_{00}^{\mathbf{q}}$) contributions for intra- or inter- band scattering with ξ, $\xi' = \pm 1$, from normal (non-magnetic) impurities at the energy $\omega = 0.2t_1$: a-d) in the normal state e-h) in the superconducting state. (Summation over each of the rows is shown in Fig.3.b and Fig.3.e).

The QPI density oscillations are obtained from the full Green's function that is determined by the effect of scattering from random charge and spin impurities at the surface. The total scattering Hamiltonian in compact form reads

$$H_{imp} = \sum_{\mathbf{k}\mathbf{q}\alpha} V_\alpha(\mathbf{q}) S_\alpha \Psi_{\mathbf{k}+\mathbf{q}}^\dagger \hat{\rho}_\alpha \Psi_{\mathbf{k}}. \qquad (3)$$

Here we use the Nambu 4-component spinor representation $\Psi^\dagger = (c_{\mathbf{k}\uparrow}^\dagger c_{\mathbf{k}\downarrow}^\dagger c_{-\mathbf{k}\uparrow} c_{-\mathbf{k}\downarrow})$. In the Nambu space the 4×4 matrices $\hat{\rho}_\alpha$ ($\alpha = (0, i) = (0, x, y, z)$) are given by $\{\hat{\rho}_\alpha\} = (\hat{\rho}_0, \hat{\boldsymbol{\rho}}) = (\tau_3\sigma_0, \tau_0\sigma_x, \tau_3\sigma_y, \tau_0\sigma_z)$. Here the τ_α- and σ_α- Pauli matrices (with $\tau_0 = \sigma_0 \equiv 1$) act on Nambu and spin indices, respectively. Furthermore we define $\{S_\alpha\} = (1, \mathbf{S})$. The first index $\alpha = 0$ corresponds to non-magnetic impurity scattering $V_0(\mathbf{q})$ and entries $i = x, y, z$ to isotropic magnetic exchange scattering $V_i(\mathbf{q}) = V_{ex}(\mathbf{q})$ from impurity spins $\mathbf{S}$. Their components S_i are treated as frozen, i.e. polarized in a given direction by a small magnetic field. An important consequence of the Rashba term is that spin and charge channels for impurity scattering are not decoupled, this also holds true for spin and charge response functions [19].

The change in STM tunneling conductance in charge or spin channel α due to impurity scattering in channel β is proportional to the resulting change of the electron Green's function [3] according to $d\delta I_\alpha(\mathbf{r}, V)/dV \sim -\frac{1}{\pi}\mathrm{Im}[\mathrm{Tr}_\sigma \hat{\rho}_\alpha \delta G_\beta(\mathbf{r}, \mathbf{r}, \omega = V)]_{11} \equiv \delta N_{\alpha\beta}(\mathbf{r}, \omega)$. Here we focus on the spatial oscillations or momentum dependence by weak scattering and ignore the possibility of bound state formation [23] in the strong scattering limit. Therefore we treat the former in Born approximation which leads to the Fourier transform of differential conductances given by

$$\delta N_{\alpha\beta}(\mathbf{q},\omega) = -\frac{1}{\pi}V_\beta(\mathbf{q})\mathrm{Im}\Big[\Lambda_{\alpha\beta}(\mathbf{q},i\omega_n)\Big]_{i\omega_n\to\omega+i\delta}, \quad (4)$$

$$\Lambda_{\alpha\beta}(\mathbf{q},i\omega_n) = \frac{1}{N}\sum_{\mathbf{k}}\mathrm{Tr}_\sigma\Big[\hat{\rho}_\alpha\hat{G}(\mathbf{k},i\omega_n)\hat{\rho}_\beta\hat{G}(\mathbf{k}-\mathbf{q},i\omega_n)\Big]_{11}$$

where $N = L^2$ is the number of grid points and indices (11) refer to the Nambu space. This expression is evaluated by using Eq. (2) and performing the trace, leads to the final result for QPI functions per spin ($\mathbf{k}' = \mathbf{k} - \mathbf{q}$)

$$\Lambda^{\mathbf{q}}_{00}(i\omega_n) = \frac{1}{4N}\sum_{\mathbf{k}\xi\xi'}\big[1+\xi\xi'(\hat{\mathbf{g}}_{\mathbf{k}}\cdot\hat{\mathbf{g}}_{\mathbf{k}'})\big]K^{\mathbf{kq}}_{\xi\xi'}(i\omega_n),$$

$$\Lambda^{\mathbf{q}}_{ii}(i\omega_n) = \frac{1}{4N}\sum_{\mathbf{k}\xi\xi'}\big[1-\xi\xi'(\hat{\mathbf{g}}_{\mathbf{k}}\cdot\hat{\mathbf{g}}_{\mathbf{k}'}-2\hat{\mathrm{g}}^{\mathrm{i}}_{\mathbf{k}}\hat{\mathrm{g}}^{\mathrm{i}}_{\mathbf{k}'})\big]\mathrm{K}^{\mathbf{kq}}_{\xi\xi'}(\mathrm{i}\omega_\mathrm{n}),$$

$$\Lambda^{\mathbf{q}}_{i0}(i\omega_n) = \frac{1}{2N}\sum_{\mathbf{k}\xi\xi'}\xi\hat{\mathrm{g}}^{\mathrm{i}}_{\mathbf{k}}\mathrm{K}^{\mathbf{kq}}_{\xi\xi'}(\mathrm{i}\omega_\mathrm{n}), \quad (5)$$

where the integration kernel for intra-band ($\xi = \xi'$) and inter-band ($\xi \neq \xi'$) processes is given by

$$K^{\mathbf{kq}}_{\xi\xi'}(i\omega_n) = \frac{(i\omega_n-\epsilon_{\mathbf{k}\xi})(i\omega_n-\epsilon_{\mathbf{k}-\mathbf{q}\xi'})-\Delta_{\mathbf{k}\xi}\Delta_{\mathbf{k}-\mathbf{q}\xi'}}{[(i\omega_n)^2-E^2_{\mathbf{k}\xi}][(i\omega_n)^2-E^2_{\mathbf{k}-\mathbf{q}\xi'}]}.$$

These equations give the QPI patterns for the NCS superconductors. Before presenting numerical results we point out the salient new features as compared to centrosymmetric unconventional superconductors [24]. Here Λ_{00} describes the charge- QPI pattern due to nonmagnetic impurities, Λ_{ii} the (diagonal) spin- QPI polarization pattern due to magnetic impurities and Λ_{i0} the spin polarization generated by *nonmagnetic* impurities which we term as cross- QPI. It occurs only for finite Rashba coupling $\mathbf{g}_{\mathbf{k}}$. The coupling of charge and spin degrees in cross- QPI appears because the Rashba band states are described by helicity and not spin quantum numbers. Therefore in general a particle-hole (charge) excitation will also change the spin state. The diagonal QPI functions in Eq. (5) are finite even for $\mathbf{g}_{\mathbf{k}} = 0$. However they are strongly modified when inversion symmetry is broken due to the Rashba helicity coherence factors in square brackets of Eq. (5) . The latter have different sign for pure charge and spin QPI functions and also change sign between intra- and interband contributions. The coherence factors can amplify or annihilate the individual contributions in the sum depending on the relative orientation of Rashba vectors and band indices. Therefore one expects that charge- ($\Lambda_{00}(\mathbf{q})$) and spin- ($\Lambda_{ii}(\mathbf{q})$) QPI pattern are profoundly different as opposed to non-Rashba case where they should be identical. The spin-QPI pattern shows a further striking Rashba effect: Although the exchange scattering itself is isotropic, $\Lambda_{ii}(\mathbf{q})$ is to be expected anisotropic in the present case when $\mathbf{g}_{\mathbf{k}}$ is confined to the tetragonal plane as seen from Eq. (5). Furthermore the Rashba term leads to nondiagonal elements in the spin- QPI pattern, in the present case to $\Lambda^{\mathbf{q}}_{xy}(i\omega_n) = \Lambda^{\mathbf{q}}_{yx}(i\omega_n)$ which is given by

$$\Lambda^{\mathbf{q}}_{xy}(i\omega_n) = \frac{1}{4N}\sum_{\mathbf{k}\xi\xi'}\xi\xi'(\hat{\mathrm{g}}^{\mathrm{x}}_{\mathbf{k}}\hat{\mathrm{g}}^{\mathrm{y}}_{\mathbf{k}-\mathbf{q}}+\hat{\mathrm{g}}^{\mathrm{y}}_{\mathbf{k}}\hat{\mathrm{g}}^{\mathrm{x}}_{\mathbf{k}-\mathbf{q}})\mathrm{K}^{\mathbf{kq}}_{\xi\xi'}(\mathrm{i}\omega_\mathrm{n}). \quad (6)$$

The QPI functions $\Lambda^{\mathbf{q}}_{00}$ and $\Lambda^{\mathbf{q}}_{ij}$ are even and $\Lambda^{\mathbf{q}}_{i0}$ is odd in $\mathbf{q}$. Therefore $\delta N_{i0}(\mathbf{r},\omega)$ is finite only when $V_0(\mathbf{q})$ contains odd (p-wave) contributions and the net (area integrated) cross-QPI conductance always vanishes.

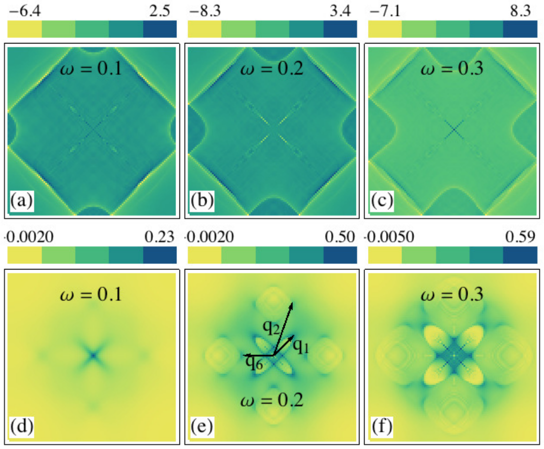

FIG. 3. a-c) Total charge- QPI ($\Lambda^{\mathbf{q}}_{00}$) in the normal state for different ω and scattering from non-magnetic impurities. d-f) The same quantity for the superconducting state. Subset ($\mathbf{q}_1, \mathbf{q}_2, \mathbf{q}_6$) of characteristic QPI wave vectors correspond to those in the spectral functions given in Fig.1.e ($\omega = 0.2t_1$).

We conclude that QPI for non-centrosymmetric superconductors derived here exhibits a wealth of new effects due to the inversion symmetry breaking Rashba term which we present now for the 2D model of 131 compounds.

All QPI spectra have four contributions from two intraband and two (equivalent) interband scattering processes. They are shown individually in Fig.2a-d for charge-QPI in the normal state and in Fig.2e-h for the SC state. In the former the scattering *across* the Fermi surface of Fig. 1b maps out the '2k$_F$' contours, partly folded back into the first BZ. They are slightly different due to the different diameter of Rashba split sheets. The diagonal center cross appears only for intraband contributions due to scattering process *parallel* to each Rashba sheet. In the SC state for small ω the sheets break up into small pieces in BZ regions connecting the node points where the gap is small. Therefore the $E_{\mathbf{k}-}$ Rashba band dominates because it is the only one with nodes (Fig.1b,e) and the SC QPI spectrum reflects the $(\xi,\xi') = (-1,-1)$ intraband transitions in Fig.2e. A set of the typical wave vectors $\mathbf{q}_i$ of Fig.1e selected by the coherence factors show

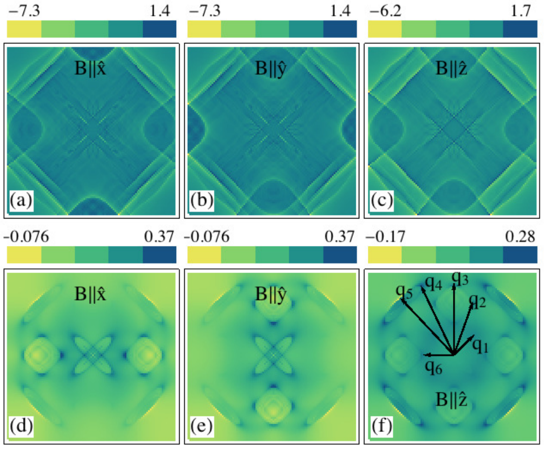

FIG. 4. a-c) Total spin- QPI ($\Lambda^{\mathbf{q}}_{ii}$) for the normal state for exchange scattering from magnetic impurities at energy $\omega = 0.2t_1$. d-f) The same quantity for the superconducting state. Each panel corresponds to different orientation of the impurity spin $\mathbf{S}$ parallel to an applied field $\mathbf{B} \to 0$. Characteristic QPI wave vectors $\mathbf{q}_i$ (Fig.1.e) are shown for $\mathbf{B} \parallel z$.

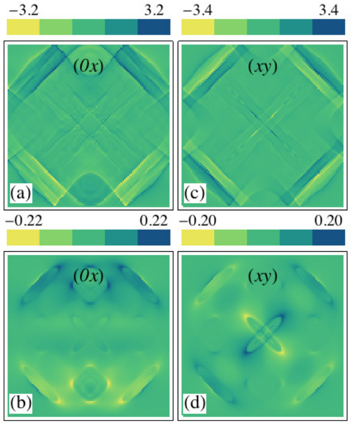

FIG. 5. a) Total cross-QPI of odd spin density $\Lambda^{\mathbf{q}}_{x0}$ in the normal state from *non-magnetic* scattering, and b) same quantity in superconducting state. c) Total non-diagonal even spin-QPI $\Lambda^{\mathbf{q}}_{xy}$ for the normal state from exchange scattering by magnetic impurities, and d) same quantity in superconducting state. Here $\mathbf{B} \to 0$ is $\parallel$ y and $\omega = 0.2t_1$.

up as prominent spots in Fig.2e. The other three contributions have lower amplitude due to the small $E_{\mathbf{k}+}$ sheets at this energy. The sum of all four contributions is the total charge-QPI spectrum which is presented in Fig.3a-f for the normal and SC state for three energies (bias voltages V): $\omega/t_1 = 0.1,\ 0.2$, and 0.3. In the former (a-c) the '$2k_F$' contours which increase with ω are now blurred due contributions with slightly different dimensions. The diagonal cross due to inraband processes appears at all energies. In the SC state for small ω the set of prominent spots at $\mathbf{q}_i$ due to Fig.2e survive and are shown explicitly in Fig.3e. The observation of these features in QPI and their variation with ω would allow to confirm directly the gap model with node structure in Fig.1b,e. For larger ω instead of spots at $\mathbf{q}_i$ arcs appear due to scattering on and between the again connected constant-ω surfaces of both Rashba bands in Fig.1h.

In the centrosymmetric superconductor ($g_{\mathbf{k}} = 0$) within Born approximation the charge- and spin- QPI functions in Eq. (5) are identical. The presence of a Rashba term introduces two new aspects due to the appearance of coherence factors (square brackets in Eq. (5)): i) the charge-and spin-QPI becomes different due to different intra-band contributions in the two cases ii) While the charge- QPI retains the fourfold symmetry as obvious from the first of Eq. (5) and Fig. 3, the spin-QPI coherence factors in the second Eq. (5) explicitly breaks rotational symmetry with respect to the impurity moment direction. This is shown in Fig.4 for normal and SC phase where we assume that a small magnetic field $\mathbf{B}$ polarizes the impurity spins $\mathbf{S}$ along one of the three symmetry directions. The spin- QPI pattern for $\mathbf{B}$ along x,y directions are still equivalent but rotated by 90°, however, both are quite different from the case $\mathbf{B} \parallel z$, in particular in the SC state. This is because in the present model the Rashba vector fulfils $\mathbf{g}_{\mathbf{k}} \cdot \hat{\mathbf{z}} = 0$ which singles out the z direction. This anisotropy of spin-QPI is therefore characteristic for non-centrosymmetric superconductors. The spin-QPI pattern is dominated by the full set of scattering vectors $\mathbf{q}_i$ connecting the high-curvature points of the constant-ω surface (Fig.4f).

Sofar we have only considered diagonal charge- or spin-QPI, however it is a very peculiar feature of NCS Rashba systems that charge-spin cross- QPI (and the reverse) described by $\Lambda^{\mathbf{q}}_{i0}$ as well as non-diagonal spin-QPI, e.g. $\Lambda^{\mathbf{q}}_{xy}$ exist. The former describes spin oscillations introduced by non-magnetic impurities (and vice versa) which are odd under inversion because $\Lambda^{-\mathbf{q}}_{i0} = -\Lambda^{\mathbf{q}}_{i0}$. It is shown in Fig.5a,b for (x0) component with spin polarization along x, again the (y0) case is just rotated in the BZ by 90° while it vanishes for (z0). Finally we show in Fig.5c,d the nondiagonal (xy) spin pattern polarized perpendicular to the impurity spins and described by Eq. (6). Only the (xy) component is non-zero because $\mathbf{g}_{\mathbf{k}}$ lies in the tetragonal plane. It also exhibits reflection symmetry with respect to diagonals (interchange of x,y directions).

We have shown that QPI in noncentrosymmetric systems exhibits a wealth of new features due to the presence of Rashba spin orbit coupling. They are important signatures of the helical spin texture and a powerful tool to investigate the nodal structure of the superconducting gap, in particular because the nodal positions are not fixed by symmetry for mixed singlet-triplet gaps.

We thank T. Takimoto for helpful comments and I. Eremin for useful discussion.

[1] K. Okazaki, Y. Ota, Y. Kotani, W. Malaeb, Y. Ishida, T. Shimojima, T. Kiss, S. Watanabe, C.-T. Chen, K. Kihou, C. H. Lee, A. Iyo, H. Eisaki, T. Saito, H. Fukazawa, Y. Kohori, K. Hashimoto, T. Shibauchi, . H. I. Y. Mat-

suda, H. Miyahara, R. Arita, A. Chainani, and S. Shin, Science **337**, 1314 (2012)

[2] Y. Matsuda, K. Izawa, and I. Vekhter, J. Phys. Condens. Matter **18**, R705 (2006)

[3] J. M. Byers, M. E. Flatté, and D. J. Scalapino, Phys. Rev. Lett. **71**, 3363 (1993)

[4] Q.-H. Wang and D.-H. Lee, Phys. Rev. B **67**, 020511 (2003)K. McElroy, R. W. Simmonds, J. E. Hoffman, D. H. Lee, J. Orenstein, H. Eisaki, S. Uchida, and J. C. Davis, Nature (London) **422**, 592 (2003)T. Hanaguri, Y. Kohsaka, M. Ono, M. Maltseva, P. Coleman, I. Yamada, M. Azuma, M. Takano, K. Ohishi, and H. Takagi, Science **323**, 923 (2009)M. Maltseva and P. Coleman, Phys. Rev. B **80**, 144514 (2009)

[5] T. Hanaguri, S. Niitaka, K. Kuroki, and H. Takagi, Science **328**, 474 (2010)T.-M. Chuang, M. P. Allan, J. Lee, Y. Xie, N. Ni, S. L. Bud'ko, G. S. Boebinger, P. C. Canfield, and J. C. Davis, *ibid.* **327**, 181 (2010)A. Akbari, J. Knolle, I. Eremin, and R. Moessner, Phys. Rev. B **82**, 224506 (2010)J. Knolle, I. Eremin, A. Akbari, and R. Moessner, Phys. Rev. Lett. **104**, 257001 (2010)

[6] A. Akbari, P. Thalmeier, and I. Eremin, Phys. Rev. B **84**, 134505 (2011)

[7] M. P. Allan, private communication

[8] P. Aynajian, E. H. da Silva Neto, C. V. Parker, Y.-K. Huang, A. Pasupathy, J. A. Mydosh, and A. Yazdani, Proc. Natl. Acad. USA **107**, 10383 (2010)

[9] A. R. Schmidt, M. H. Hamidian, P. Wahl, F. Meier, A. V. Balatsky, J. D. Garrett, T. J. Williams, G. M. Luke, and J. C. Davis, Nature **465**, 570 (2010)

[10] T. Yuan, J. Figgins, and D. K. Morr, Phys. Rev. B **86**, 035129 (2012)

[11] R. Settai, T. Takeuchi, and Y. Onuki, J. Phys. Soc. Jpn **76**, 051003 (2007)

[12] E. Bauer, H. Kaldarar, A. Prokofiev, E. Royanian, A. Amato, J. Sereni, W. Brämer-Escamilla, and I. Bonalde, J. Phys. Soc. Jpn **76**, 051009 (2007)

[13] N. Kimura, Y. Muro, and H. Aoki, J. Phys. Soc. Jpn **76**, 051010 (2007)

[14] P. A. Frigeri, D. F. Agterberg, I. Milat, and M. Sigrist, Eur. Phys. J. B **54**, 435 (2006)

[15] I. Eremin and J. F. Annett, Phys. Rev. B **74**, 184524 (2006)

[16] S. Fujimoto, J. Phys. Soc. Jpn **76**, 051008 (2007)

[17] K. V. Samokhin, E. S. Zijlstra, and S. K. Bose, Phys. Rev. B **69**, 094514 (2004)

[18] M. Sigrist, "Introduction to unconventional superconductivity in non-centrosymmetric superconductors," (American Institute of Physics, 2009) Chap. CP1162, pp. 55–97

[19] T. Takimoto, J. Phys. Soc. Jpn **77**, 113706 (2008)

[20] T. Takimoto and P. Thalmeier, J. Phys. Soc. Jpn **78**, 103703 (2009)

[21] Y. Yanase and M. Sigrist, J. Phys. Soc. Jpn **77**, 124711 (2008)

[22] K. Izawa, Y. Kasahara, Y. Matsuda, K. Behnia, T. Yasuda, R. Settai, and Y. Onuki, Phys. Rev. Lett. **94**, 197002 (2005)

[23] B. Liu and I. Eremin, Phys. Rev. B **78**, 014518 (2008)

[24] L. Capriotti, D. J. Scalapino, and R. D. Sedgewick, Phys. Rev. B **68**, 014508 (2003)